HHS Public Access

Author manuscript

Eur J Neurosci. Author manuscript; available in PMC 2015 June 19.

Published in final edited form as:

Eur J Neurosci. 2012 February ; 35(3): 389–401. doi:10.1111/j.1460-9568.2011.07978.x.

The influence of single bursts vs. single spikes at excitatory dendrodendritic synapses

Arjun V. Masurkar[1,*] and **Wei R. Chen**[1,2]

[1]Department of Neurobiology, Yale University School of Medicine, New Haven, CT, USA

[2]Department of Neurobiology and Anatomy, University of Texas Medical School, Houston, TX, USA

Abstract

The synchronization of neuronal activity is thought to enhance information processing. There is much evidence supporting rhythmically bursting external tufted cells (ETCs) of the rodent olfactory bulb glomeruli coordinating the activation of glomerular interneurons and mitral cells via dendrodendritic excitation. However, as bursting has variable significance at axodendritic cortical synapses, it is not clear if ETC bursting imparts a specific functional advantage over the preliminary spike in dendrodendritic synaptic networks. To answer this question, we investigated the influence of single ETC bursts and spikes with the *in-vitro* rat olfactory bulb preparation at different levels of processing, via calcium imaging of presynaptic ETC dendrites, dual electrical recording of ETC–interneuron synaptic pairs, and multicellular calcium imaging of ETC-induced population activity. Our findings supported single ETC bursts, vs. single spikes, driving robust presynaptic calcium signaling, which in turn was associated with profound extension of the initial monosynaptic spike-driven dendrodendritic excitatory postsynaptic potential. This extension could be driven by either the spike-dependent or spike-independent components of the burst. At the population level, burst-induced excitation was more widespread and reliable compared with single spikes. This further supports the ETC network, in part due to a functional advantage of bursting at excitatory dendrodendritic synapses, coordinating synchronous activity at behaviorally relevant frequencies related to odor processing *in vivo*.

Keywords

bursting; circuitry; olfaction; rat; synapse

Introduction

The olfactory glomeruli are important processing modules in the mammalian olfactory bulb (OB). Spatial patterns of activated glomeruli encode odor identity (Stewart et al. 1979). Each glomerulus is a functional unit, where homogeneous sensory input to output neurons,

Correspondence: Arjun V. Masurkar, *present address below. avm2114@columbia.edu.

**Present address*: Neurological Institute of New York, 710 West 168th Street, Columbia University Medical Center, New York, NY 10032-3784, USA

mitral and tufted cells is modulated by interneurons, periglomerular cells (PGCs) and short axon cells (Mombaerts et al. 1996; Shepherd et al. 2004; Chen and Shepherd, 2005).

How is intraglomerular processing coordinated? Evidence *in vivo* suggests that the input drive and intrinsic circuits influence OB temporal activity patterns (Sobel and Tank, 1993). The input is modulated by dopamine and GABA (Aroniadou-Anderjaska et al. 2000; Ennis et al. 2001; Wachowiak and Cohen, 1999; Wachowiak et al. 2005; McGann et al. 2005; Shao et al. 2009), possibly from a rhythmically active interneuron subtype (Puopolo et al. 2005; Pignatelli et al. 2005; Maher and Westbrook, 2008; Kiyokage et al. 2010). The mitral and tufted cells are synchronized by multiple mechanisms (Isaacson, 1999; Schoppa and Westbrook, 2001; Christie et al. 2005; Christie and Westbrook, 2006; De Saint Jan et al. 2009; Najac et al 2011). Interneurons are coordinated by external tufted cells (ETCs), which are superficial output neurons at the deep glomerular borders.

The ETCs extend expansive dendrites mostly to single glomeruli and fire rhythmic bursts consisting of slow calcium plateau potentials supporting multiple sodium spikes (McQuiston and Katz, 2001; Hayar et al. 2004a; Zhou et al. 2006a; Antal et al. 2006; Liu and Shipley, 2008; Masurkar and Chen, 2011b). The ETCs excite PGCs and short axon cells within a glomerulus (Hayar et al. 2004b; Murphy et al. 2005; Kiyokage et al. 2010), whereas GABAergic input from PGCs controls ETC excitability (Hayar et al. 2005; Gire and Schoppa 2009). ETCs also excite mitral cells (De Saint Jan et al 2009; Najac et al 2011), whereas feedback excitation and/or glutamate spillover modulate ETC excitability (Hayar et al. 2005). ETCs themselves are mutually electrically coupled (Hayar et al. 2005). Thus, the relationship between the ETCs and other glomerular neurons is complex but critical to coordinating the glomerular processing ultimately represented in mitral and tufted cell activity.

Interestingly, ETC bursts trigger large, long duration postsynaptic depolarizations in glomerular interneurons (Hayar et al., 2004b) and also depolarizations or multiple spikes in mitral cells (De Saint Jan et al 2009; Najac et al 2011). It is unclear if this excitation is elicited specifically by the burst or by extended effects of the preliminary spike, as burst firing is of variable significance at cortical axodendritic synapses due to short-term plasticity, postsynaptic conductances, passive summation, and recruitment of excitatory and/or inhibitory circuits (Thomson, 2000; Krahe and Gabianni, 2004; Izhikevich et al. 2003). Furthermore, the effects of bursts compared with spikes within glomeruli may be unexpected because of action at dendrodendritic synapses, and within a highly interconnected network of such dendritic processes, gap junctions, and axons that define the glomerular circuits.

Here, we used several approaches with *in-vitro* rat OB slice preparations to examine the functional impact of single ETC bursts vs. spikes at the level of the presynaptic dendrite, postsynaptic potential, and small neuronal populations.

Materials and methods

This study was approved by our institutional review board for animal research, the Yale University Animal Care and Use Committee.

Slice preparation

Sprague-Dawley rats (*Rattus norvegicus*), 12-21 days old, were anesthetized with 1.2 g/kg urethane (Sigma, USA) intraperitoneally until unresponsive to tail pinch, and decapitated according to Yale University Animal Care and Use Committee guidelines. The OBs were extracted in chilled (4 °C) and oxygenated (95% O_2, 5% CO_2) artificial cerebrospinal fluid (ACSF). The ACSF contained 124 mM NaCl, 2 mM $CaCl_2$, 3 mM KCl, 1.25 mM NaH_2PO_4, 26 mM $NaHCO_3$, 1.3 mM $MgSO_4$, and 10 mM dextrose at pH 7.4. Horizontal slices of 400 μm thickness were made using a rotorslicer (Dosaka, Japan) and immediately immersed in an oxygenated ACSF bath at 34 °C for 15-20 min. Slices were then kept in oxygenated ACSF at room temperature for up to 8 h.

Bicuculline was prepared as a stock solution dissolved in high pH ACSF adjusted with KOH. D-APV, 6-cyano-7-nitroquinoxaline-2,3-dione, saclofen, LY341495, and tetrodotoxin (TTX) were prepared as stock solutions in ddH_2O. All stock solutions were stored under refrigeration except TTX, which was stored at −20 °C. All chemical reagents were from Sigma unless otherwise specified.

Current-clamp recordings of external tufted cells

Cells were recorded in whole-cell mode. The intracellular solution consisted of 130 mM K-gluconate, 10 mM HEPES, 0.2 mM EGTA, 4 mM MgATP, 0.3 mM Na_3GTP, and 10 mM Na_2phosphocreatine, adjusted to pH 7.3-7.4 with KOH. In our laboratory, we have traditionally used this solution, which contains no exogenous chloride ions, to amplify inhibition and have obtained stable recordings in mitral cells (Chen et al. 1997), granule cells (Xiong and Chen, 2002), and ETCs (Zhou et al. 2006a). The ACSF used for slice preparation was the same as that used for recordings. All experiments in this study were performed at 33-37 °C by heating ACSF using a TC-344B temperature controller (Warner Instruments, New Haven, CT, USA).

Cells were visually identified with an infrared camera (Hamamatsu, Japan, C2400-07ER) on an upright microscope (Olympus, BX50WI) using differential interference contrast microscopy and a 40× water immersion objective. ETCs were identified as cells having the largest somata at the deep glomerular border, most often with the dendritic trunk extending into the glomerulus. Current-clamp whole-cell recordings were made using Axoclamp 2A and 2B amplifiers (Axon Instruments, Union City, CA, USA) in bridge-balance current-clamp mode and Pclamp 9.0 for acquisition. Data were sampled at 10-20 kHz. Recording pipettes were pulled from 1.20 mm outer diameter/0.69 mm inner diameter glass with a P-97 Flaming/Brown micropipette puller (Sutter Instruments, San Rafael, CA, USA), with final resistances of 8-12 MΩ.

The olfactory nerve was stimulated by placing a large-tip pipette (1 MΩ) filled with ACSF or a concentric bipolar stimulating electrode (25 μm diameter tip) on the olfactory nerve

layer surface; each of these was connected to an electrical isolator that controlled the current amplitude of stimulation. The nerve was stimulated with one shock (0.05-0.2 ms width, 0.1 mA or less).

Single external tufted cell calcium imaging

For single-cell calcium imaging, 50 μM Calcium Green-1 hexapotassium salt (Invitrogen) was added to the intracellular solution. The dye was allowed to diffuse throughout the neuron for 15-20 min after entering whole-cell mode before starting the experiment.

For imaging, slices were epilluminated via a 150 W xenon arc lamp (Opti-Quip, Highland Mills, NY, USA) through a 460-500 nm excitation filter (HQ480/40x, Chroma Technology Corp., Bellows Falls, VT, USA) and dichroic mirror (Chroma Technology Corp., Q505LP). Fluorescence was collected by a 510-560 nm emission filter (Chroma Technology Corp., HQ535/50m). The fluorescence emission was captured by a PentaMax frame-transfer cooled CCD camera (Princeton Instruments, Trenton, NJ, USA) using Axon Imaging Workbench 2.2 (Axon Instruments). A 25 Hz frame rate was used and imaging was performed with an ND filter (¼) in the excitation path to decrease photobleaching and phototoxicity and allow more imaging trials. For analysis, monoexponential photobleaching was assumed and subtracted out postacquisition. Trials comparing spikes and bursts were interleaved and then averaged.

External tufted cell–interneuron paired recordings

Interneurons were recorded in the same manner as ETCs by targeting electrodes to smaller somata at the glomerular border. Pairs were found by random double-patch recordings of ETCs and smaller interneuron somata thought to be projecting primary dendrites to the same glomerulus. A synaptic connection was confirmed if postsynaptic depolarization with monosynaptic delay was evident after averaging a minimum of five trials of postsynaptic membrane potential recording in response to presynaptic suprathreshold activity. Subsets of interneurons, as described in the text, were anatomically indistinguishable, although single-spike-firing neurons had much smaller somata.

Multicellular calcium imaging of population responses to single external tufted cell stimulation

Slices were prepared as above and then stained with Oregon Green 488 BAPTA-1 or Calcium Green-1 (Invitrogen), both in acetoxymethyl (AM) ester form, using a double-labeling protocol (Peterlin et al. 2000) as follows. The AM dyes were prepared by dissolving 50 μg dye in 1% Pluronic F-127 (Invitrogen), 5% dimethylsulfoxide, and 5% Cremaphor-EL in a total volume of 100 μL pluronic and dimethylsulfoxide stock as a combination of 20% Pluronic in 100% dimethylsulfoxide. The slices, after the 34 °C incubation step above, were placed in individual wells of a well plate. A small volume (20 μL) of AM dye stock solution (387 μM for CG-1 AM) was placed on each slice and they remained in this solution for 2 min. Subsequently, 2 mL of oxygenated ACSF was added to each well to dilute the dye stock 100× to a final concentration of 3.87 μM CG-1 AM, 0.01% Pluronic F-120, 0.05% dimethylsulfoxide, and 0.05% Cremaphor-EL. Well plates were immediately transferred to a

tissue culture incubator (37 °C) for 30 min, and then placed back in the regular oxygenated ACSF bath for 30 min until imaging experiments commenced.

The ETCs were targeted and recorded as above. The experiments were again performed at 33-37 °C. In these experiments, Mg^{2+} was left out of the ACSF. Fluorescence imaging was performed as described earlier but the ¼ ND filter was not used. To limit photodamage, and thus false-negative results, we instead limited our imaging trials to less than 10. A 20 Hz frame rate was used.

For analysis, regions of interest (ROIs) that corresponded to soma-sized areas in all glomeruli were examined. Monoexponential photobleaching was assumed and subtracted out postacquisition. Trials comparing spikes and bursts were interleaved. Responses were considered successful only if clearly distinguishable from noise. The timings of calcium responses were correlated with electrophysiology, allowing one time frame of error. Responses that were more delayed were not counted. Responses showing very slow rises in ΔF/F (a τ_{rise} of seconds) were probably of glial origin and those (ROIs) were not included.

Statistical analysis

Statistical analysis was performed with QuickCalcs (GraphPad Software Inc., La Jolla, CA, USA). All analyses comprised simple comparisons of two means with SEs, each representing the same variable measured under different experimental conditions, with small sample sizes. Therefore, a non-directional Student's t-test was chosen for the determination of significance, and results are reported with the *t*-statistic value, with degrees of freedom as subscript, followed by the *P*-value. The significance criterion was $P < 0.05$. Numerical averages are presented in figures with SE values, and within the text as ± SD. Within-subject (same acute slice) factors were mainly associated with averaging interneuron measurements or ETC measurements, in that interneurons are known to be heterogeneous and ETCs may be heterogeneous themselves. Between-subject factors (different acute slices, different animals) include subtle connectivity or population differences at various depths of the OB and the age range of animals used (see above).

Results

External tufted cell dendritic calcium signals are driven more robustly by bursts and plateau potentials than spikes

The ETCs were located by their large somata and position at the deep border of glomeruli (Fig. 1A). ETC bursts, which were elicited by and outlasted short depolarizing current pulses, consisted of two components, fast spikes and a slow plateau potential (“1” and “2”, Fig. 1Bi). To probe the influence of an entire ETC burst, we established two manipulations to evaluate the independent functional contributions of the fast and slow components. The initial spike was readily isolated from the burst by a brief hyperpolarizing pulse following the initial depolarizing current pulse (Fig. 1Bii, top inset). The plateau potential, which was probably driven by T-type calcium conductance (McQuiston and Katz, 2001; Hayar et al., 2004a; Zhou et al. 2006a; Liu and Shipley, 2008; Masurkar and Chen, 2011b), was isolated with 1 μM TTX to block fast sodium channels (Fig. 1Biii, bottom inset).

Based on electron microscopy evidence, ETCs have been proposed to excite glomerular interneurons largely via dendrodendritic synapses, although evidence also exists for ETC axon collaterals in the glomeruli (Pinching and Powell, 1971a; Pinching and Powell, 1971b). Numerous physiological studies have subsequently supported glutamate release from ETC dendrites to dendrites of other glomerular interneurons and mitral cells (Hayar et al., 2004b; Murphy et al., 2005; De Saint Jan et al., 2009; Gire and Schoppa, 2009; Najac et al., 2011). If ETC dendrites house functional presynaptic terminals, we questioned whether the tuft could support sufficient depolarization to mediate dendritic transmitter release. Employing fluorescence imaging of calcium influx as a surrogate marker of depolarization, our previous study found that ETC bursts could elicit calcium signals in the distal dendrite, whereas single spikes could not (Zhou et al., 2006b). However, the ultrastructure supports that it is the more proximal medium- and large-caliber processes that carry presynaptic vesicles to participate in dendrodendritic synapses (Pinching and Powell, 1971b; Kasowski et al. 1999). We focused our experimentation on this region of the tuft and also extended this work to assess calcium influx in the complete absence of Na^+ spikes.

We first tested if and where single ETC bursts and action potentials could elicit a dendritic calcium signal. ETCs were loaded with Calcium Green-1 calcium indicator (0.05 mM) via the patch pipette. Figure 2A shows a typical indicator-filled ETC with somatic (1) and secondary branch (2 and 3) ROIs labeled. Both a burst and single spike could elicit responses (ΔF/F) in the soma as well as in visualized dendritic locations (Fig. 2Bi and ii, respectively, n = 10). Overall, when detected, spike- and burst-induced calcium signals were widespread and not branch-specific. Both signals reduced in amplitude along the somatodendritic axis, but with burst-induced transients having much larger amplitudes (Fig. 2C; n = 13 total; $t_{22} = 4.23$, $P = 0.0003$; $t_{21} = 4.43$, $P = 0.0002$; $t_{17} = 4.15$, $P = 0.007$; $t_7 = 2.49$, $P = 0.042$ at soma, trunk, primary branches, and secondary branches, respectively).

The enhanced dendritic depolarization by bursts could be due to additional intraburst spike content. To evaluate this, in a subgroup of the above experiments, we repeated imaging with all spikes blocked by 1 μM TTX. The remaining plateau potential could also drive large calcium transients in the soma and dendrites (Fig. 2D, n = 6). Such signals were significantly larger than measurable spike-induced signals (Fig. 2E, blue; $t_4 = 4.12$, $P = 0.015$; $t_5 = 7.09$, $P = 0.0009$; $t_4 = 9.15$, $P = 0.0008$; $t_4 = 6.12$, $P = 0.0036$ at soma, trunk, primary branches, and secondary branches, respectively) and similar in amplitude to burst-induced signals (Fig. 2E, black; $t_5 = 2.56$, $P = 0.048$ at soma but $t_5 = 0.50$, $P = 0.64$; $t_4 = 0.71$, $P = 0.52$; $t_3 = 0.86$, $P = 0.45$ at trunk, primary branches, and secondary branches, respectively). At minimum these data implied that the enhanced ability of bursts to elevate intradendritic calcium is due to concurrent effects by the additional spike content as well as independently by the underlying plateau potential. If we assume that the indicator was not saturated, furthermore it appeared that the calcium plateau potential contributed more to intradendritic calcium influx than the multiple sodium spikes.

To rule out whether enhanced signaling by bursts is due to the activation of recurrent excitation or inhibition, which could ETC electrical excitability (Hayar et al., 2005; De Saint Jan and Westbrook, 2007; Ma and Lowe, 2007; Hayar and Ennis, 2007; Karpuk and Hayar, 2008; Dong et al. 2009; De Saint Jan et al., 2009; Najac et al., 2011), we repeated these

experiments with block of synaptic transmission. Again, bursts induced larger signals than single spikes in the presence of antagonists of ionotropic (APV/6-cyano-7-nitroquinoxaline-2,3-dione/bicuculline, n = 6, Fig. 2F) and metabotropic (saclofen and LY341495, in addition to ionotropic receptor blockade, n = 2, Supporting Information Fig. 1) receptors. Notably, however, the ratio between burst- and spike-induced signals was reduced compared with controls at all levels tested, although this was only statistically significant at the soma (n = 6; $t_{16} = 3.36$, $P = 0.016$ at soma; $t_{15} = 0.90$, $P = 0.38$; $t_{10} = 1.66$, $P = 0.13$ at trunk and primary branches, respectively; only one sample for secondary branch signal with synaptic transmission blockers). This suggested that enhanced calcium signaling by ETC bursts is mediated by intrinsic mechanisms of increased calcium entry but may also be influenced by recruitment of recurrent and/or spillover-related excitation. Indeed, this could be derived from Ca^{2+}-permeable AMPA receptors (Ma and Lowe, 2007) as well as from recurrent or spillover pathways activating metabotropic glutamate receptor-mediated calcium influx derived from internal stores and Ca^{2+}-dependent non-specific cation conductance (Dong et al. 2009).

External tufted cell bursts elicit robust and large monosynaptic excitation of interneurons

Regardless of the mechanism, if bursts, spikes, and plateau potentials induce dendritic calcium signals, does this correlate with dendritic transmitter release? Also, is the enhanced calcium entry by bursts and plateau potentials necessarily associated with enhanced transmitter release compared with single spikes? The next series of experiments examined these questions. We first searched for synaptic connections between ETCs and smaller glomerular neurons, presumed to be interneurons, with dendrites projecting to the same glomerulus (Fig. 3A). Out of 151 dual whole-cell recordings between ETCs and interneurons, 26 synaptic pairs were identified, all showing unidirectional excitatory transmission from ETC to interneuron. All ETCs generated similar appearing postsynaptic depolarizations, delineated below, in three interneuron types based on their firing pattern (Supporting Information Fig. 2).

The firing patterns were based on responses to a long, square current injection into many, but not all, of the postsynaptic cells. We observed a multiple-spiking type (Supporting Information Fig. 2A and B, n = 3), a bursting type (Supporting Information Fig. 2C and D, n = 3), and another subgroup firing only a single spike (Supporting Information Fig. 2E and F, n = 10). Although the sample size was small, these postsynaptic cells resembled some previously characterized firing types of rodent PGCs (Puopolo and Belluzzi, 1998; McQuiston and Katz, 2001; Pignatelli et al., 2005; Puopolo et al., 2005; Zhou et al. 2006a). Although the postsynaptic cells were hyperpolarized to prevent overt spontaneous activity and to record subthreshold input from ETCs, occasional spontaneous firing was observed in the latter two categories, as has been observed in studies of other PGCs (McQuiston and Katz, 2001; Pignatelli et al., 2005; Puopolo et al., 2005; Zhou et al. 2006a).

The ETC bursts elicited complex, large-amplitude, long-duration depolarizations in these postsynaptic neurons (Fig. 3B, black, n = 26). The average amplitude of this postsynaptic potential was 7.3±4.1 mV and its half-maximal duration was 38.0±22.0 ms (n = 15, only pairs stable for multiple trials were selected for analysis and pharmacology). Such

depolarizations were glutamatergic excitatory postsynaptic potentials (EPSPs), eliminated by the addition of the AMPA and *N*-methyl-D-aspartate receptor (NMDAR) blockers 6-cyano-7-nitroquinoxaline-2,3-dione and APV, respectively (Fig. 3C, n = 2). The average delay between the peak of the first presynaptic spike and the start of the EPSP was consistent with some monosynaptic dendrodendritic excitation (0.52±0.19 ms, n = 15). The burst-induced output was of extraordinarily high fidelity, with a release probability (P_r) of 1.0 (n = 15).

What caused such large and robust EPSPs? Despite the delay, which was suggestive of a monosynaptic component, was any component directly related to transmitter release from the presynaptic ETC and not solely an intermediary excitatory neuron? The chelation of internal calcium with 20 mM EGTA in the patch pipette hastened the decay of the EPSP magnitude over several minutes of dialysis (Fig. 3D), and similar results were obtained with 5-20 mM BAPTA (Fig. 3E), suggesting that at least some of the postsynaptic depolarization was due to transmitter release coupled to calcium influx into the presynaptic ETC.

External tufted cell burst-induced output is enhanced by spike-dependent and spike-independent glutamate release

We next tested whether the large burst-induced depolarization was due to mechanisms triggered only by the initial presynaptic action potential or by the entire burst itself. We first isolated the contribution of the preliminary spike of the ETC burst to the EPSP in interneurons. This postsynaptic potential was a smaller amplitude, shorter duration EPSP that corresponded to the first component of the burst-induced EPSP (Fig. 3B, blue). Indeed, the amplitude of the first component of the burst-induced EPSP and the amplitude of the spike-induced EPSP were not statistically different (Fig. 3F, $t_{37} = 1.19$, $P = 0.24$ for one pair, shown, similar for all tested pairs, n = 7). The spike-mediated output alone also had a high P_r of 0.93±0.18 (Fig. 3G, n = 8, $t_{14} = 1.12$, $P = 0.28$ compared with burst P_r). Over most pairs, the average amplitude of the first spike-induced EPSP peak was smaller than the total peak of the burst-induced EPSP (Fig. 3H, n = 13, $t_{24} = 3.42$, $P = 0.011$). To quantify this intraburst facilitation, we measured this EPSP amplitude gain across these pairs, which was 2.6±1.4 (n = 13). This enhancement could be due to the facilitation of transmitter release, recruitment of polysynaptic excitatory pathways, activation of gap junction pathways, active summation via postsynaptic conductances, and/or passive summation. Any of these mechanisms could be triggered by either the additional sodium spikes of the burst or the underlying calcium plateau potential. We attempted to make postsynaptic recordings in voltage-clamp mode to more carefully assess the postsynaptic summation but were unable to maintain stable recordings.

Instead, we next aimed to assess the function of the additional spikes by generating ETC spike trains without evoking the calcium plateau potential, and recorded the postsynaptic EPSP that they produced (Fig. 3I, n = 5). As shown, such spikes, generated maximally at approximately 80 Hz, could also evoke a large EPSP. Although it was difficult to exactly compare this spike train with the spikes within ETC bursts, which numbered two to four at a frequency of 251± 99 Hz (n = 32), this suggested that multiple spikes could generate a large postsynaptic depolarization similar to that generated by the burst.

We next evaluated if the large EPSPs evoked by ETC bursts could also be mediated by the calcium current-mediated plateau potential. To assess the contribution of the plateau potential to the postsynaptic responses, in a subset of ETC–interneuron synaptic pair dual recordings, we added 2 μM TTX extracellularly to eliminate fast Na^+ spikes (n = 4). The EPSPs persisted and were large in amplitude (Fig. 4A, blue) and generated with a P_r of 1.0 (n = 4). No membrane voltage deflections were elicited by the capacitative transient alone (Fig. 4A, green). Within individual trials, the EPSPs typically had a time course that followed the activation of plateau potential (Fig. 4B). This led to an average synaptic delay that was significantly elevated (Fig. 4C, $t_6 = 8.45$, $P = 0.0002$) and with a variability that was much increased when compared with burst-induced EPSPs containing sodium action potentials (Fig. 4D, $t_6 = 7.04$, $P = 0.0004$). The overall area of the burst-induced EPSPs was slightly larger than that of plateau potential-induced EPSPs, but this difference was not significant (Fig. 4E, $t_8 = 0.66$, $P = 0.53$).

Taken together, these results support that large burst-induced EPSPs are partly due to glutamatergic transmitter release by the presynaptic ETC, and that the extension of the initial monosynaptic EPSP is generated by the subsequent sodium spikes and/or the calcium plateau potential. It appears that the spike-mediated output maintains more temporal precision, in that the synaptic delay is more deterministic. The persistence of large EPSPs in the presence of TTX lessens the likelihood that action potential-dependent polysynaptic pathways and postsynaptic amplifications dependent on fast sodium conductance contribute to the extension of the EPSP. Furthermore, the elimination of the potential with chelation of presynaptic calcium, and the absence of voltage deflections in the postsynaptic cell in proportion to those in the ETC lessened the likelihood that direct electrical coupling between ETCs and interneurons was playing a role. Therefore, the extension of the spike-induced depolarization is due to further monosynaptic transmitter release, activation of polysynaptic glutamatergic dendrodendritic pathways, gap junction effects via intermediary neurons that are dependent on glutamatergic excitation, and/or other postsynaptic conductances such as calcium channels.

A single external tufted cell burst excites multiple glomerular interneurons restricted to the same glomerulus

With evidence that ETC bursts excite single interneurons more than single spikes, we then tested whether this effect translated to the population level. Multicellular calcium imaging experiments have established that single ETCs can excite multiple PGCs (Murphy et al. 2005), as well as multiple mitral cells (De Saint Jan et al. 2009). We explored whether a single ETC burst could activate glomerular cell populations more efficiently than a single ETC spike. To achieve multicellular activity recording, we employed the bulk loading of calcium indicator (Oregon Green-488 BAPTA-1 AM or Calcium Green-1 AM) in slices and used somatic calcium signals (ΔF/F) as surrogate markers for electrical activity (Peterlin et al. 2000). The uptake of calcium indicator was seen in multiple neuronal somata in the glomerular layer (Fig. 5Ai and Bi). A burst was elicited in single ETCs while simultaneously recording ΔF/F in ROIs at the glomerular and cellular level in response to this stimulation. The intracellular solution did not contain calcium indicator so as to only

record the postsynaptic calcium responses and not calcium transients from the stimulated ETC. Any uptake in the patched ETC was diluted by dialysis with intracellular solution.

Surprisingly, we were unable to elicit any response transients in interneurons with this technique with extracellular magnesium present in the recording solution, but obtained robust transients when extracellular magnesium was excluded. This suggested that, in our preparation, the network effects of the ETC burst were dependent on NMDAR-mediated mechanisms. We explored this hypothesis in experiments discussed in this and the following section in parallel to establishing the effects of a single burst and spike within this “excited” network,

To first elucidate in which layers of the OB the ETC bursts elicited calcium responses, we focused our analysis on large areas in the external plexiform layer (EPL), glomerular layer, and olfactory nerve layer. In the example shown in Fig. 5Ai, the dashed boxes demarcate these ROIs, with two glomeruli (A and B) indicated. We assumed that such a bulk signal was due to contributions by multiple activated somata and activated processes comprising the neuropil. In this example, ETC X (labeled in Fig. 5Ai, black traces in Fig. 5Aii), thought to belong to glomerulus A based on extension of the dendritic trunk, was stimulated with current injection to elicit one burst. In a single trial, this burst was associated with a calcium transient in glomerulus A and not glomerulus B, the EPL, or olfactory nerve layer (Fig. 5Aii, right colored traces). Over all experiments, fluorescence transients in response to a single ETC burst were limited to the glomerular layer and, more specifically, were in the glomerulus to which the stimulated ETC belonged (Fig. 5Aiii, n = 11, $t_{28} = 6.24$, $P < 0.0001$). This contrasts with reports of single ETC bursts exciting mitral cells (De Saint Jan et al. 2009), which would have predicted some signal in the EPL and mitral cell layer. In our preparations, we noted little uptake of indicator in mitral cell primary dendrites and mitral cell bodies once the calcium indicator incubation was completed, similar to another study (Murphy et al. 2005).

We then focused our analysis at single cell level. Figure 5Bi shows the same example as in Fig. 5A with interneuron ROIs highlighted. Cells were identified by soma-sized punctate labeling at rest. In a single trial, when one ETC (cell X) burst was elicited via current injection, calcium signals in multiple somata were recorded. As indicated by the colored circles (red, responder; blue, non-responder), activated interneurons were restricted to a common glomerulus, and the same glomerulus to which the ETC belonged (Fig. 5Bii). For further evidence that these ROIs were somata and not heterogeneous neuropil, we confirmed the uniformity of responses at the pixel level for the ROIs (Supporting Information Fig. 3A shown for cell 14). Note that one ETC burst does not excite all cells in the glomerulus (blue outlined cells in glomerulus A). The average maximum number of cells that one ETC burst activated in a trial, per experiment, was 5.5±3.7 cells (n = 13), similar to that reported in another study in which ETC spikes were generated with a slightly different stimulus (Murphy et al. 2005).

As the interglomerular borders were assumed based on interpretation of the DIC microscope image of the slice landscape, we measured the distance between activated interneurons and the trigger ETC X for all experiments (Fig. 5Biii, n = 6). Responding interneurons were

distributed with distances at or less than the glomerular diameter of 100-150 μm in rat (Meister and Bonhoeffer, 2001). Although there are reports of ETC subtypes having dendrites extending to multiple glomeruli or exciting glutamatergic short axon cells that project to other glomeruli, which could confound the interpretation of this number (Antal et al. 2006; Kiyokage et al. 2010), this distance distribution matches our observation of calcium signals limited to a single glomerulus. Nevertheless, this spatial distribution, as well as the example in Fig. 5B, also indicated that activated interneurons were distributed at various distances from the stimulated ETC, including those towards the olfactory nerve layer and EPL. Therefore, it was unlikely that activated neurons represented only other ETCs residing at the EPL–glomerular border that were electrically coupled to the trigger ETC (Hayar et al. 2005).

As mentioned above, we hypothesized that the postsynaptic calcium transients elicited were probably dependent on NMDAR-dependent pathways. First, the transients themselves could be representative of subthreshold electrical events or from spiking. The NMDARs could enhance calcium signals from either electrical event via direct calcium influx, enhanced depolarization due to non-specific cation influx, and/or recruitment of polysynaptic pathways. To further assess this, we first established that ETC burst-triggered interneuron somatic signals were indeed sensitive to blockade by the NMDAR antagonist APV (Supporting Information Fig. 3B). Then, in slices without bulk calcium indicator present, we directly loaded glomerular interneurons with 50 μM Calcium Green-1 calcium indicator via recording pipettes and imaged the somatic ΔF/F in response to subthreshold and suprathreshold activity. Across all of the interneuron physiological subtypes (as in Supporting Information Fig. 2), subthreshold input via olfactory nerve stimulation did not elicit somatic calcium signals, whereas suprathreshold activity elicited by current injection did generate somatic calcium transients (Supporting Information Fig. 3C, n = 4 or 5 per interneuron category). Our interpretation was that it was most probable that postsynaptic spikes were also required to visualize postsynaptic calcium transients. Therefore, our interpretation is that the postsynaptic calcium signals induced by single ETC bursts visualized in our multicellular imaging experiment represented calcium influx that was reliant on spiking activity and NMDAR-mediated mechanisms. At this juncture, we could not exclude a role for polysynaptic pathways induced by NMDAR activation in our Mg^{2+}-free preparation, or rule out enhanced excitation of the presynaptic ETC dendrite in these conditions. The latter, and other related issues, is addressed in conjunction with our results in the next section.

External tufted cell bursts are more efficient in the delivery of widespread excitation than single external tufted cell spikes

To test if burst firing was more effective at eliciting such multicellular responses than spike firing, we repeated these slice calcium imaging experiments and compared single ETC bursts with single ETC spikes. Another example of calcium indicator-loaded slices is shown in Fig. 6A. One ETC (X) was stimulated to fire a single spike by current injection, and 500 ms later a burst was elicited in the same trial (Fig. 6Bi and ii, bottom). The interneuron somatic ΔF/F was recorded in response to these two waveforms. Two trials are shown, with responses from multiple cells, in Fig. 6Bi and ii. In Fig. 6Bi, the spike activated only cell A,

whereas the burst excited cells A and B. In another trial (Fig. 6Bii), the spike again excited only cell A, whereas the burst excited all four cells (A-D). Therefore, beyond the enhanced excitement of single cells, bursting increased the number of interneurons activated by an ETC vs. a single spike. Based on the above discussion, this could have been derived from enhanced monosynaptic or polysynaptic events that are dependent on NMDAR-mediated mechanisms.

This effect was probably due in part to an increase in the probability of exciting individual interneurons. To assess this, we examined the responsiveness of single cells over multiple trials. Using the same example (Fig. 6A), cell A was excited by the spike in three out of five trials, whereas the burst was effective in all trials (Fig. 6Ci). As shown in Fig. 6Cii, cell D was activated in two out of five trials by the burst and in none by the spike.

These two effects were seen quantitatively over all experiments. We calculated the degree of coactivity imparted by an ETC as a percent of all responsive interneurons activated in a trial, per experiment. An ETC burst induced more coactivity than a single spike from the same ETC (Fig. 6D, n = 6; $t_{10} = 2.76$, $P = 0.02$). We also calculated the average interneuron response probability as the percent of trials in which a given interneuron was responsive over the total trial number. Interneurons showed a higher response probability with single ETC bursts than single ETC spikes (Fig. 6E; n = 32; $t_{62} = 6.46$, $P < 0.0001$). Responses to either waveform were not weighted to earlier trials, and testing single spikes vs. burst in separate trials led to similar results (not shown).

Part of this enhancement by ETC bursts was possibly due to increased NMDAR-mediated activity in our magnesium-free condition. To test this, we again performed synaptic pair recordings between ETC–interneuron pairs, as in Fig. 3, but this time in zero extracellular magnesium. We were able to confirm that spike-induced EPSPs were similarly smaller than burst-induced EPSPs (Supporting Information Fig. 4A, n = 3). However, compared with conditions with magnesium included, the EPSP due to the first ETC spike, the peak of the entire burst-induced EPSP, and the total EPSP half-maximal duration appeared larger, although only the EPSP comparison was significant (Supporting Information Fig. 4Bi, $t_{16} = 1.09$, $P = 0.29$; Supporting Information Fig. 4Bii, $t_{16} = 2.81$, $P = 0.013$; Supporting Information Fig. 4Biii, $t_{16} = 1.72$, $P = 0.11$, respectively). Therefore, the enhanced ability of ETC bursts to excite multiple neurons, compared with spikes, in the absence of extracellular magnesium, was partially due to larger postsynaptic potentials that were probably enhanced due to NMDAR-mediated mechanisms.

Part of this enhancement by ETC bursts was also possibly due to the increased NMDAR-mediated excitation of the presynaptic ETC dendrite, as we alluded to its sensitivity to glutamate spillover or recurrent excitation in Fig. 2. We repeated our experiments presented in Fig. 2, this time in zero extracellular magnesium. The ETC intradendritic calcium elevations by bursts and spikes indeed showed similar patterning (Supporting Information Fig. 4C; n = 5; $t_8 = 4.62$, $P = 0.0017$; $t_8 = 4.29$, $P = 0.0027$; $t_7 = 3.42$, $P = 0.011$ at soma, trunk, and primary branches, respectively; only one cell with a secondary branch). Furthermore, comparing these presynaptic ETC calcium signals with conditions with magnesium present (Fig. 2), the calcium influx was enhanced only at the dendritic shaft

when elicited by bursts (t_{24} = 2.42, P = 0.024), where presynaptic vesicles are less likely to be housed (Pinching and Powell, 1971b; Kasowski et al. 1999). Therefore, in our magnesium-free preparation, the enhanced network effects of an ETC burst compared with an ETC spike were less likely to be due to enhanced presynaptic excitability, but more likely to be due to enhanced monosynaptic or polysynaptic pathways dependent on NMDARs.

Discussion

In this study we compared ETC bursts and spikes at the level of presynaptic calcium entry, postsynaptic depolarization in individual cells, and small neuronal populations. Burst firing caused enhanced tuft-wide presynaptic calcium entry compared with single spikes, probably augmented by influx guided by the spike-independent plateau potential underlying the burst, and possibly supplemented by recurrent excitation or spillover mechanisms. This, in turn, was associated with large, long duration monosynaptic EPSPs elicited in the postsynaptic interneuron, to which both the presynaptic spikes and plateau potential contributed. Multicellular imaging suggested that these effects translated to the population level, with an ETC burst more robustly promoting synchronous activation of small populations of glomerulus-specific interneurons, albeit in an excitable preparation.

Excitability of external tufted cell dendrites

Our evidence for small spike-induced calcium transients in the proximal dendritic processes, depreciating along the somatodendritic axis, is not inconsistent with our previous findings that spikes do not elicit signals in the distal tuft (Zhou et al. 2006b). Furthermore, spike-mediated calcium transients in the proximal part of the arbor, given the location of presynaptic vesicles in the ETC dendrite (Pinching and Powell, 1971b; Kasowski et al., 1999), are consistent with our demonstration that single ETC spikes cause monosynaptic EPSPs. This is in contrast to mitral cells, in which the distal processes can support robust calcium signaling due to spikes (Charpak et al. 2001; Xiong and Chen, 2002; Christie and Westbrook, 2003; Zhou et al. 2006b). As in hippocampal pyramidal neurons (Jaffe et al 1992), such profound depreciation is conceivably due to insufficient Na^+ channel density, as opposed to Ca^{2+} channel deficiency, as ETC bursts induce measurable distal calcium entry (Zhou et al. 2006b).

Our finding of four- to fivefold larger, burst-induced calcium signals in these proximal portions of the dendritic arbor also extends previous evidence of such signals in the distal ETC dendrite (Zhou et al 2006b). The functional relevance of this enhancement is evident in our recordings of larger, more robust EPSPs driven by bursts compared with single spikes. What generates the enhancement? Plateau potentials induced similarly large signals, although we cannot definitively conclude that they mediated the majority of the burst-induced signal due to the possibility of indicator saturation. However, given that plateau potential-induced signals were three to four times the magnitude of spike-induced signals in the same compartment and that contributions to intradendritic calcium elevation by additional spikes in a train are severely sublinear (Spruston et al. 1995; Callaway and Ross, 1995) or linear at best (Zhou et al. 2006b), it is unlikely that spikes contribute significantly to the ETC burst-induced dendritic calcium influx. Furthermore, mitral cells possess a

dendritic A-type potassium current that attenuates action potentials along the dendrite and limits spike-induced dendritic calcium transients (Christie and Westbrook, 2003) and there is evidence that ETCs also possess a significant A-type potassium current (Liu and Shipley, 2008; Masurkar and Chen 2011a).

Our results suggest that the mechanism by which the burst and/or plateau potential could enhance intradendritic presynaptic calcium influx is via both enhanced intrinsic calcium entry and recruitment of excitatory circuits (recurrent or spillover-related). Considering the intrinsic mechanisms, pronounced calcium transients elicited by the subthreshold plateau potential make it possible that this was due to calcium entry via T-type calcium channels, which mediates the plateau potential (McQuiston and Katz, 2001; Zhou et al. 2006a; Liu and Shipley, 2008; Masurkar and Chen, 2011b). Indeed, evidence supports a dendritic location for these channels, as the evolution of the ETC burst is prevented by a puff of nickel, a non-specific T-type calcium current blocker, at the dendrite of the ETC (Zhou et al. 2006a).

Enhanced postsynaptic depolarization by a burst vs. a single spike via spike-dependent and -independent mechanisms

Bursts may not necessarily enhance synaptic transmission compared with spikes for various reasons. These include presynaptic mechanisms, e.g. inefficient propagation of spikes/depolarizations to the presynaptic terminal, reduced presynaptic calcium influx, saturation of the calcium sensor, and exhaustion of vesicle pools. They also include postsynaptic mechanisms such as postsynaptic receptor saturation, shunting or hyperpolarizing postsynaptic conductances, or recruitment of feedforward or feedback inhibition. Many of these mechanisms could be relevant to the ETC–interneuron dendrodendritic synapse, in that ETC presynaptic function is inherently sensitive to the excitability of its dendrites based on anatomy (Pinching and Powell, 1971b; Kasowski et al. 1999), ETCs are poised to receive feedback inhibition (Hayar et al. 2004b; Murphy et al. 2005; Hayar et al. 2005; Karpuk and Hayar, 2008; Gire and Schoppa 2009; Kiyokage et al. 2010), and PGCs are known to possess hyperpolarization-activated and A-type potassium currents (Cadetti and Belluzzi, 2001; Pupolo and Belluzzi, 1998) that can reduce or shunt EPSPs. Furthermore, we noted that the single spike-induced output from ETCs was extraordinarily high in amplitude and probability, similar to olfactory nerve (Murphy et al. 2004), and typically synapses with a high P_r display rapid depression of spike-induced output (Dobrunz and Stevens, 1997; Abbott and Regehr, 2004).

However, bursts induced even larger EPSPs than single spikes, as found at many, but not all, axodendritic synapses (Thomson, 2000; Krahe and Gabianni, 2004; Izhikevich et al. 2003). Both the plateau potential and multiple spikes of the burst appeared to be able to elicit this enhancement on their own.

Part of this may be due to presynaptic mechanisms, including the promotion of unattenuated depolarization to the terminal, increased calcium signaling, more efficient mobilization of transmitter, and activation of more unitary synapses. Multiple sodium spikes may penetrate the presynaptic dendrite more efficiently than a single spike, despite the evidence to the contrary in multiple cell types (Spruston et al. 1995; Callaway and Ross, 1995; Zhou et al. 2006b). Secondly, we have shown profound calcium signaling due to the plateau potential

itself, which may in turn enhance transmitter release. It would be interesting to examine whether the spikes and plateau potential stimulate the same or different transmitter vesicles, or stimulate release from a common pool coupled to different calcium channels and sensors. Indeed, in other neurons, transmitter release is coupled to various calcium channels with differing efficiency (Mintz et al. 1995; Wu et al. 1999). The efficient delivery of excitation by spike trains and calcium plateau potential also imply an inherent redundancy to the delivery of excitation by ETC bursts to interneurons, as the number of spikes per burst is sensitive to the balance of excitation and inhibition (Hayar and Ennis, 2007; Karpuk and Hayar, 2008; Dong et al. 2009) and the T-type current is modulated by the metabotropic glutamatergic input, at least in mitral cells (Johnston and Delaney, 2010).

As mentioned above, we also could not rule out that such enhancement could be due to many postsynaptic mechanisms. This includes feedforward and feedback excitatory pathways, many of which have been demonstrated to be related to principal neurons of the OB, including ETCs (Isaacson, 1999; Friedman and Strowbridge, 2000; Schoppa and Westbrook, 2002; Lowe, 2003; Hayar et al., 2005; De Saint Jan and Westbrook, 2007; Ma and Lowe, 2007; Dong et al. 2009; De Saint Jan et al., 2009; Najac et al., 2011). This could also be related to intermediary gap junction mechanisms that are also known to exist (Kosaka and Kosaka, 2003; Hayar et al 2005). It should also be noted that autoinhibition in the glomerulus can be depolarizing, and therefore excitation from the ETC to the interneuron could also be enhanced by recurrent inhibition activated by the postsynaptic GABAergic interneuron (Smith and Jahr, 2003). This was minimized in our experiments by not including chloride in our intracellular solutions. Although we ruled out that postsynaptic sodium channels were likely to not play a role, given that EPSPs were large even with TTX applied, we could not comment on whether postsynaptic calcium conductances could also amplify the EPSP. Indeed, PGCs have been shown to possess both low-threshold and high-threshold calcium channels of unknown localization (Murphy et al., 2005; Pignatelli et al., 2005; Puopolo et al., 2005).

The presence of both action potential-dependent and action potential-independent mechanisms to excite glomerular interneurons contrasts with the finding of only fast Na^+ channel-dependent excitation of mitral cells by ETCs (De Saint Jan et al. 2009). This EPSP was reliable but very short in duration, suggesting that it was driven by a single spike, and the authors could not rule out that AMPA-mediated autoexcitation was playing a role. The difference in these mechanisms is suggestive of differences in excitatory synaptic connectivity between ETCs and interneurons compared with ETCs and mitral cells. For example, excitation driven by the Ca^{2+}-mediated plateau potential may be more efficiently spread to interneurons if it activates a different pool of presynaptic vesicles that happens to be more associated with interneurons than mitral cells. Plateau potential-based depolarization may be more easily spread to intermediary excitatory neurons via gap junctions, as alluded to above. There may also be more activation of NMDAR-dependent polysynaptic pathways from the ETC to interneurons compared with ETC to mitral cells.

The effect of external tufted cells on population-level responses in the olfactory bulb

Multiple studies support the critical role of synchronous neural activity in processing within neuronal networks (Engel et al. 2001). Divergent excitation by a rhythmic oscillator is a proposed mechanism of such synchrony (Ritz and Sejnowski, 1997), making the ETC network an attractive locus for intraglomerular correlated activity. As discussed earlier, ETCs are mutually electrically coupled (Hayar et al., 2005), excite multiple types of glomerular interneuron (Hayar et al., 2004a; Hayar et al. 2004b; Murphy et al. 2005; Kiyokage et al. 2010), and single bursts have been shown to excite small populations of glomerular interneurons and mitral cells (Murphy et al., 2005; De Saint Jan et al. 2009; Najac et al. 2011).

Our experiments expand on these previous studies, in the context of comparing single ETC bursts with single spikes. It appears that the robust synaptic transmission induced by single ETC bursts translates to more widespread and consistent excitation compared with the single spike. We acknowledge that our multicellular preparation was limited by the requirement to exclude extracellular magnesium to elicit detectable responses. Other studies have demonstrated ETC-induced calcium transients in both interneurons (Murphy et al. 2005) and mitral cells (De Saint Jan et al. 2009) with extracellular magnesium present. However, to compare, in the former study, the approach used was to depolarize the ETC to produce five or more action potentials via a square voltage-clamp step impulse (Murphy et al. 2005). In our experiments, we wished to functionally analyze the naturally evolving ETC burst in current clamp, which typically featured only two to four sodium spikes that often did not surpass 0 mV when recorded at the soma. Furthermore, it may also be that endogenous glutamate may become depleted with the preparation, as multiple studies have turned instead to supplying ETCs with exogenous glutamate in the intracellular solution (Murphy et al. 2005; Ma and Lowe, 2007; De Saint Jan et al. 2009; Najac et al. 2011). We did not want to supply exogenous glutamate because some larger non-glutamatergic PGCs fire bursts similar to ETCs (McQuiston and Katz, 2001; Zhou et al., 2006a) and, if inadvertently targeted, could cause false secretion of glutamate instead of dopamine and/or GABA (Dan et al. 1994), perturbing the interpretation of network effects. Alternatively, we aimed to maintain the same intracellular solution as for our paired recordings, and chose instead to more carefully examine the effects of our magnesium manipulation, as delineated in the Results.

Regarding these, using our multiple control experiments, we were at least able to support that triggered somatic calcium responses probably reflected the spiking activity enhanced by NMDAR-mediated mechanisms, which certainly included prolongation of the EPSP, and this NMDAR effect was probably more pronounced at the postsynaptic level (monosynaptic or polysynaptic) rather than reflecting enhanced excitation of the presynaptic ETC dendrite itself.

Furthermore, one could consider a physiological source for this relief of magnesium block of the NMDAR deriving from a secondary source for excitation within the glomerular network, either from continual olfactory nerve sensory input, mitral/tufted cell dendritic glutamate release, or electrical coupling from other depolarized neuronal elements. Placed within this framework, our results may reflect that burst-induced population excitation is

more sensitive to enhancement by these concurrent excitatory inputs than is population excitation by single spikes.

Despite the potential strength of rhythmic excitation from a network of ETC bursts, the glomerular network also possesses other neuronal oscillators. These include the autorhythmic dopaminergic interneurons (Puopolo et al. 2005; Pignatelli et al. 2005) that may comprise an important recurrent inhibitory feedback circuit (via GABA and dopamine corelease) to the very olfactory sensory input that drives ETCs (Aroniadou-Anderjaska et al. 2000; Ennis et al. 2001; Wachowiak and Cohen, 1999; Wachowiak et al. 2005; McGann et al. 2005; Maher and Westbrook, 2008). Interestingly, dopaminergic cells are often disynaptically excited by ETCs and not directly by sensory input (Shao et al. 2009; Kiyokage et al. 2010). There are also PGCs that fire spontaneous low-threshold bursts (McQuiston and Katz, 2001; Zhou et al. 2006a), although their neurochemical identity is unclear. Therefore, diverse rhythmically active circuits intimately influence the total effect of the ETC network on glomerular processing, and this is worthy of further study. However, by being an excitatory element, the ETC network may be the critical amplifier of input drive to initiate synchronous intraglomerular activity.

Summary

These results suggest that the population effect of single bursts compared with spikes in excitatory dendrodendritic networks is similar to that found in hippocampal (Csicsvari et al. 1998) and thalamocortical (Beierlein et al. 2002) networks that are hallmarked by axodendritic connections. Furthermore, this is certainly in line with the more widespread and large calcium signaling evoked in the presynaptic dendritic arbor by the ETC burst. The increased reliability is consistent with the ability of presynaptic bursts to bring postsynaptic neurons closer to spiking threshold more robustly and for a longer period of time than single spikes, which was also demonstrated in our experiments above. Overall, this work further supports that the ETC network, in part specifically via the burst firing mode, can control local glomerular synchrony and could, in turn, exert tremendous influence on odorant processing in the OB.

Supplementary Material

Refer to Web version on PubMed Central for supplementary material.

Acknowledgments

We thank Drs S. Nagayama, M. Fletcher, W. Xiong, F. Jia, and Z. Zhou for discussion and technical assistance. We thank Dr G. Shepherd for guidance. This work was supported by the National Institute of Deafness and Other Communication Disorders [Grants DC-003918, DC-009666 (W.R.C.), and DC-004732 (G. M. Shepherd)], and also a National Institutes of Health Medical Scientist Training Program Grant (A.V.M.).

References

Abbott LF, Regehr WG. Synaptic computation. Nature. 2004; 431:796–803. [PubMed: 15483601]

Antal M, Eyre M, Finklea B, Nusser Z. External tufted cells in the main olfactory bulb form two distinct subpopulations. Eur J Neurosci. 2006; 24:1124–1136. [PubMed: 16930438]

Aroniadou-Anderjaska V, Zhou FM, Priest CA, Ennis M, Shipley MT. Tonic and synaptically evoked presynaptic inhibition of sensory input to the rat olfactory bulb via GABA(B) heteroreceptors. J Neurophysiol. 2000; 84:1194–1203. [PubMed: 10979995]

Beierlein M, Fall CP, Rinzel J, Yuste R. Thalamocortical bursts trigger recurrent activity in neocortical networks: layer 4 as a frequency-dependent gate. J Neurosci. 2002; 22:9885–9894. [PubMed: 12427845]

Cadetti L, Belluzzi O. Hyperpolarisation-activated current in glomerular cells of the rat olfactory bulb. Neuroreport. 2001; 12:3117–3120. [PubMed: 11568648]

Callaway JC, Ross WN. Frequency-dependent propagation of sodium action potentials in dendrites of hippocampal CA1 pyramidal neurons. J Neurophysiol. 1995; 74:1395–1403. [PubMed: 8989380]

Charpak S, Mertz J, Beaurepaire E, Moreaux L, Delaney K. Odor-evoked calcium signals in dendrites of rat mitral cells. Proc Natl Acad Sci USA. 2001; 98:1230–1234. [PubMed: 11158622]

Chen WR, Midtgaard J, Shepherd GM. Forward and backward propagation of dendritic impulses and their synaptic control in mitral cells. Science. 1997; 278:463–467. [PubMed: 9334305]

Chen WR, Shepherd GM. The olfactory glomerulus: a cortical module with specific functions. J Neurocytol. 2005; 34:353–360. [PubMed: 16841172]

Christie JM, Bark C, Hormuzdi SG, Helbig I, Monyer H, Westbrook GL. Connexin36 mediates spike synchrony in olfactory bulb glomeruli. Neuron. 2005; 46:761–772. [PubMed: 15924862]

Christie JM, Westbrook GL. Regulation of backpropagating action potentials in mitral cell lateral dendrites by A-type potassium currents. J Neurophysiol. 2003; 89:2466–2472. [PubMed: 12740404]

Christie JM, Westbrook GL. Lateral excitation within the olfactory bulb. J Neurosci. 2006; 26:2269–2277. [PubMed: 16495454]

Csicsvari J, Hirase H, Czurko A, Buzsaki G. Reliability and state dependence of pyramidal cell-interneuron synapses in the hippocampus: an ensemble approach in the behaving rat. Neuron. 1998; 21:179–189. [PubMed: 9697862]

Dan Y, Song HJ, Poo MM. Evoked neuronal secretion of false transmitters. Neuron. 1994; 13:909–917. [PubMed: 7946337]

De Saint Jan D, Hirnet D, Westbrook GL, Charpak S. External tufted cells drive the output of olfactory bulb glomeruli. J Neurosci. 2009; 29:2043–2052. [PubMed: 19228958]

De Saint Jan D, Westbrook GL. Disynaptic amplification of metabotropic glutamate receptor 1 responses in the olfactory bulb. J Neurosci. 2007; 27:132–140. [PubMed: 17202480]

Dobrunz LE, Stevens CF. Heterogeneity of release probability, facilitation, and depletion at central synapses. Neuron. 1997; 18:995–1008. [PubMed: 9208866]

Dong HW, Hayar A, Callaway J, Yang XH, Nai Q, Ennis M. Group I mGluR activation enhances Ca(2+)-dependent nonselective cation currents and rhythmic bursting in main olfactory bulb external tufted cells. J Neurosci. 2009; 29:11943–11953. [PubMed: 19776280]

Engel AK, Fries P, Singer W. Dynamic predictions: oscillations and synchrony in top-down processing. Nat Rev Neurosci. 2001; 2:704–716. [PubMed: 11584308]

Ennis M, Zhou FM, Ciombor KJ, Aroniadou-Anderjaska V, Hayar A, Borrelli E, Zimmer LA, Margolis F, Shipley MT. Dopamine D2 receptor-mediated presynaptic inhibition of olfactory nerve terminals. J Neurophysiol. 2001; 86:2986–2997. [PubMed: 11731555]

Friedman D, Strowbridge BW. Functional role of NMDA autoreceptors in olfactory mitral cells. J Neurophysiol. 2000; 84:39–50. [PubMed: 10899181]

Gire DH, Schoppa NE. Control of on/off glomerular signaling by a local GABAergic microcircuit in the olfactory bulb. J Neurosci. 2009; 29:13454–13464. [PubMed: 19864558]

Hayar A, Ennis M. Endogenous GABA and glutamate finely tune the bursting of olfactory bulb external tufted cells. J Neurophysiol. 2007; 98:1052–1056. [PubMed: 17567771]

Hayar A, Karnup S, Ennis M, Shipley MT. External tufted cells: a major excitatory element that coordinates glomerular activity. J Neurosci. 2004; 24:6676–6685. [PubMed: 15282270]

Hayar A, Karnup S, Shipley MT, Ennis M. Olfactory bulb glomeruli: external tufted cells intrinsically burst at theta frequency and are entrained by patterned olfactory input. J Neurosci. 2004; 24:1190–1199. [PubMed: 14762137]

Hayar A, Shipley MT, Ennis M. Olfactory bulb external tufted cells are synchronized by multiple intraglomerular mechanisms. J Neurosci. 2005; 25:8197–8208. [PubMed: 16148227]

Isaacson JS. Glutamate spillover mediates excitatory transmission in the rat olfactory bulb. Neuron. 1999; 23:377–384. [PubMed: 10399942]

Izhikevich EM, Desai NS, Walcott EC, Hoppensteadt FC. Bursts as a unit of neural information: selective communication via resonance. Trends Neurosci. 2003; 26:161–167. [PubMed: 12591219]

Jaffe DB, Johnston D, Lasser-Ross N, Lisman JE, Miyakawa H, Ross WN. The spread of Na+ spikes determines the pattern of dendritic Ca2+ entry into hippocampal neurons. Nature. 1992; 357:244–246. [PubMed: 1350327]

Johnston J, Delaney KR. Synaptic activation of T-type Ca2+ channels via mGluR activation in the primary dendrite of mitral cells. J Neurophysiol. 2010; 103:2557–2569. [PubMed: 20071628]

Karpuk N, Hayar A. Activation of postsynaptic GABAB receptors modulates the bursting pattern and synaptic activity of olfactory bulb juxtaglomerular neurons. J Neurophysiol. 2008; 99:308–319. [PubMed: 18032562]

Kasowski HJ, Kim H, Greer CA. Compartmental organization of the olfactory bulb glomerulus. J Comp Neurol. 1999; 407:261–274. [PubMed: 10213094]

Kiyokage E, Pan YZ, Shao Z, Kobayashi K, Szabo G, Yanagawa Y, Obata K, Okano H, Toida K, Puche AC, Shipley MT. Molecular identity of periglomerular and short axon cells. J Neurosci. 2010; 30:1185–1196. [PubMed: 20089927]

Kosaka T, Kosaka K. Neuronal gap junctions in the rat main olfactory bulb, with special reference to intraglomerular gap junctions. Neurosci Res. 2003; 45:189–209. [PubMed: 12573466]

Krahe R, Gabbiani F. Burst firing in sensory systems. Nat Rev Neurosci. 2004; 5:13–23. [PubMed: 14661065]

Liu S, Shipley MT. Multiple conductances cooperatively regulate spontaneous bursting in mouse olfactory bulb external tufted cells. J Neurosci. 2008; 28:1625–1639. [PubMed: 18272683]

Lowe G. Flash photolysis reveals a diversity of ionotropic glutamate receptors on the mitral cell somatodendritic membrane. J Neurophysiol. 2003; 90:1737–1746. [PubMed: 12724365]

Ma J, Lowe G. Calcium permeable AMPA receptors and autoreceptors in external tufted cells of rat olfactory bulb. Neuroscience. 2007; 144:1094–1108. [PubMed: 17156930]

Maher BJ, Westbrook GL. Co-transmission of dopamine and GABA in periglomerular cells. J Neurophysiol. 2008; 99:1559–1564. [PubMed: 18216231]

Masurkar AV, Chen WR. Potassium currents of olfactory bulb juxtaglomerular cells: characterization, simulation, and implications for plateau potential firing. Neuroscience. 2011a; 192:247–262. [PubMed: 21704678]

Masurkar AV, Chen WR. Calcium currents of olfactory bulb juxtaglomerular cells: profile and multiple conductance plateau potential simulation. Neuroscience. 2011b; 192:231–246. [PubMed: 21704681]

McGann JP, Pirez N, Gainey MA, Muratore C, Elias AS, Wachowiak M. Odorant representations are modulated by intra- but not interglomerular presynaptic inhibition of olfactory sensory neurons. Neuron. 2005; 48:1039–1053. [PubMed: 16364906]

McQuiston AR, Katz LC. Electrophysiology of interneurons in the glomerular layer of the rat olfactory bulb. J Neurophysiol. 2001; 86:1899–1907. [PubMed: 11600649]

Meister M, Bonhoeffer T. Tuning and topography in an odor map on the rat olfactory bulb. J Neurosci. 2001; 21:1351–1360. [PubMed: 11160406]

Mintz IM, Sabatini BL, Regehr WG. Calcium control of transmitter release at a cerebellar synapse. Neuron. 1995; 15:675–688. [PubMed: 7546746]

Mombaerts P, Wang F, Dulac C, Chao SK, Nemes A, Mendelsohn M, Edmondson J, Axel R. Visualizing an olfactory sensory map. Cell. 1996; 87:675–686. [PubMed: 8929536]

Murphy GJ, Darcy DP, Isaacson JS. Intraglomerular inhibition: signaling mechanisms of an olfactory microcircuit. Nat Neurosci. 2005; 8:354–364. [PubMed: 15696160]

Murphy GJ, Glickfeld LL, Balsen Z, Isaacson JS. Sensory neuron signaling to the brain: properties of transmitter release from olfactory nerve terminals. J Neurosci. 2004; 24:3023–3030. [PubMed: 15044541]

Najac M, De Saint Jan D, Reguero L, Grandes P, Charpak S. Monosynaptic and polysynaptic feed-forward inputs to mitral cells from olfactory sensory neurons. J Neurosci. 2011; 31:8722–8729. [PubMed: 21677156]

Peterlin ZA, Kozloski J, Mao BQ, Tsiola A, Yuste R. Optical probing of neuronal circuits with calcium indicators. Proc Natl Acad Sci USA. 2000; 97:3619–3624. [PubMed: 10737806]

Pignatelli A, Kobayashi K, Okano H, Belluzzi O. Functional properties of dopaminergic neurones in the mouse olfactory bulb. J Physiol. 2005; 564:501–514. [PubMed: 15731185]

Pinching AJ, Powell TP. The neuron types of the glomerular layer of the olfactory bulb. J Cell Sci. 1971a; 9:305–345. [PubMed: 4108056]

Pinching AJ, Powell TP. The neuropil of the glomeruli of the olfactory bulb. J Cell Sci. 1971b; 9:347–377. [PubMed: 4108057]

Puopolo M, Bean BP, Raviola E. Spontaneous activity of isolated dopaminergic periglomerular cells of the main olfactory bulb. J Neurophysiol. 2005; 94:3618–3627. [PubMed: 16033943]

Puopolo M, Belluzzi O. Functional heterogeneity of periglomerular cells in the rat olfactory bulb. Eur J Neurosci. 1998; 10:1073–1083. [PubMed: 9753175]

Ritz R, Sejnowski TJ. Synchronous oscillatory activity in sensory systems: new vistas on mechanisms. Curr Opin Neurobiol. 1997; 7:536–546. [PubMed: 9287205]

Schoppa NE, Westbrook GL. Glomerulus-specific synchronization of mitral cells in the olfactory bulb. Neuron. 2001; 31:639–651. [PubMed: 11545722]

Schoppa NE, Westbrook GL. AMPA autoreceptors drive correlated spiking in olfactory bulb glomeruli. Nat Neurosci. 2002; 5:1194–1202. [PubMed: 12379859]

Shao Z, Puche AC, Kiyokage E, Szabo G, Shipley MT. Two GABAergic intraglomerular circuits differentially regulate tonic and phasic presynaptic inhibition of olfactory nerve terminals. J Neurophysiol. 2009; 101:1988–2001. [PubMed: 19225171]

Shepherd, GM., et al. Olfactory bulb. In: Shepherd, GM., editor. Synaptic Organization of the Brain. Oxford; New York: 2004. p. 165-216.

Smith TC, Jahr CE. Self-inhibition of olfactory bulb neurons. Nat Neurosci. 2002; 5:760–766. [PubMed: 12089528]

Sobel EC, Tank DW. Timing of odor stimulation does not alter patterning of olfactory bulb unit activity in freely breathing rats. J Neurophysiol. 1993; 69:1331–1337. [PubMed: 8492167]

Spruston N, Schiller Y, Stuart G, Sakmann B. Activity-dependent action potential invasion and calcium influx into hippocampal CA1 dendrites. Science. 1995; 268:297–300. [PubMed: 7716524]

Stewart WB, Kauer JS, Shepherd GM. Functional organization of rat olfactory bulb analysed by the 2-deoxyglucose method. J Comp Neurol. 1979; 185:715–734. [PubMed: 447878]

Thomson AM. Molecular frequency filters at central synapses. Prog Neurobiol. 2000; 62:159–196. [PubMed: 10828382]

Wachowiak M, Cohen LB. Presynaptic inhibition of primary olfactory afferents mediated by different mechanisms in lobster and turtle. J Neurosci. 1999; 19:8808–8817. [PubMed: 10516300]

Wachowiak M, McGann JP, Heyward PM, Shao Z, Puche AC, Shipley MT. Inhibition [corrected] of olfactory receptor neuron input to olfactory bulb glomeruli mediated by suppression of presynaptic calcium influx. J Neurophysiol. 2005; 94:2700–2712. [PubMed: 15917320]

Wu LG, Westenbroek RE, Borst JG, Catterall WA, Sakmann B. Calcium channel types with distinct presynaptic localization couple differentially to transmitter release in single calyx-type synapses. J Neurosci. 1999; 19:726–736. [PubMed: 9880593]

Xiong W, Chen WR. Dynamic gating of spike propagation in the mitral cell lateral dendrites. Neuron. 2002; 34:115–126. [PubMed: 11931746]

Zhou Z, Xiong W, Masurkar AV, Chen WR, Shepherd GM. Dendritic calcium plateau potentials modulate input-output properties of juxtaglomerular cells in the rat olfactory bulb. J Neurophysiol. 2006a; 96:2354–2363. [PubMed: 16855116]

Zhou Z, Xiong W, Zeng S, Xia A, Shepherd GM, Greer CA, Chen WR. Dendritic excitability and calcium signalling in the mitral cell distal glomerular tuft. Eur J Neurosci. 2006b; 24:1623–1632. [PubMed: 17004926]

Abbreviations

ACSF	artificial cerebrospinal fluid
AM	acetoxymethyl
EPL	external plexiform layer
EPSP	excitatory postsynaptic potential
ETC	external tufted cell
NMDAR	*N*-methyl-D-aspartate receptor
OB	olfactory bulb
PGC	periglomerular cell
P_r	release probability
ROI	region of interest
TTX	tetrodotoxin

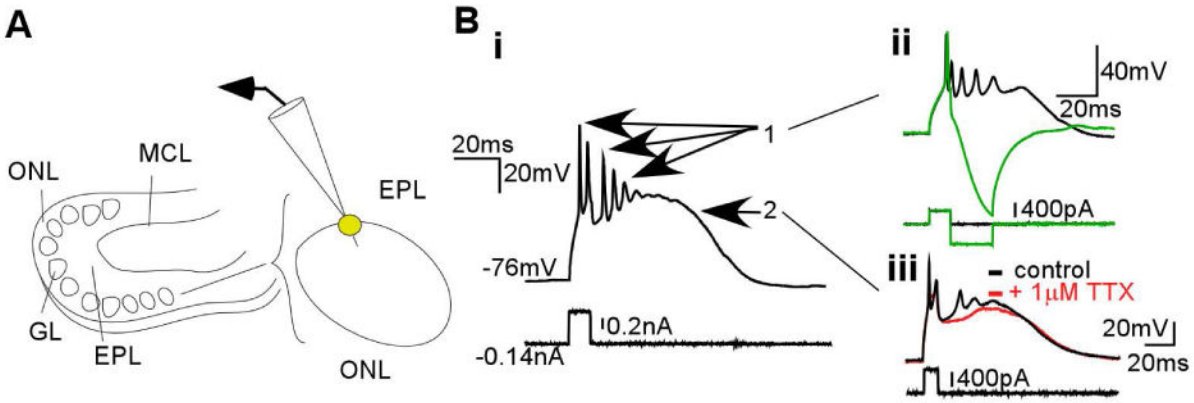

Fig. 1.

ETCs at the deep glomerular border fire bursts consisting of a plateau potential supporting multiple Na^+ spikes. (A) Illustration of a horizontal rat OB slice, with olfactory nerve layer (ONL), glomerular layer (GL), EPL, and mitral cell layer (MCL) labeled to the left. As on the right, recordings were performed on ETCs, which were identified as large somata at the GL–EPL border. (B) Current-clamp recordings of an ETC burst (i) consisted of two separable components: (ii) fast spikes, of which the initial large spike could be separated with a hyperpolarizing pulse to block the rest of the burst, and (iii) a plateau potential that could be separated from spikes with TTX.

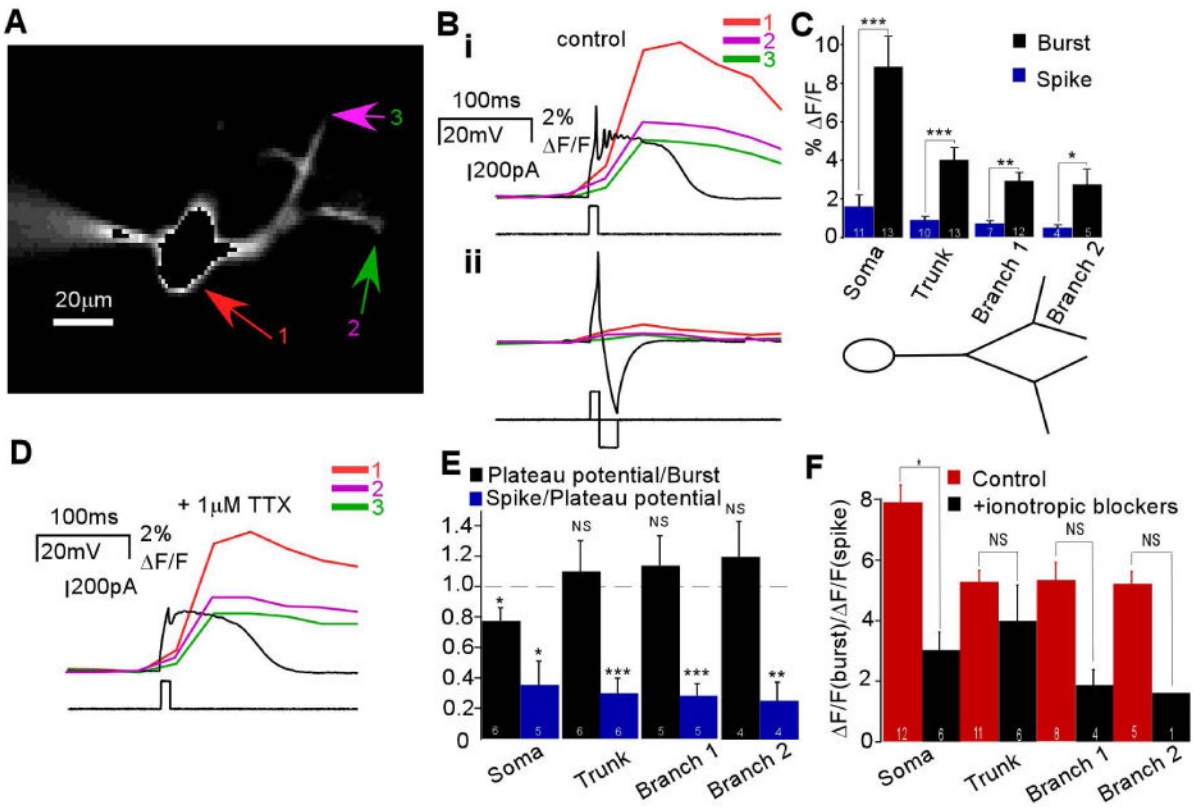

Fig. 2.

Calcium influx into ETC dendrites is more robustly mediated by bursts and plateau potentials than single spikes. (A) Fluorescence image of an ETC cell filled intracellularly with 50 μM Calcium Green-1; arrows indicate three ROIs: soma (1), secondary branch in the bottom part of the arbor (2) and secondary branch in the top part of the arbor (3). (B) (i) Bursts evoked large fluorescence signals (ΔF/F) in all three locations (top), whereas a single spike (ii) evoked a much smaller response (bottom) (n = 13). (C) Burst- and spike-induced calcium signals depreciated across the somatodendritic axis but burst-induced signals were significantly larger (n as indicated; **P*<0.05, ***P*<0.01, ****P*<0.0005). (D) With Na^+ spikes blocked by TTX, a plateau potential evoked a large calcium signal in the three locations defined above (n = 6). (E) Beyond the soma, the ratio between burst- and spike-induced calcium signals (left) was close to 1 across the somatodendritic axis (n as indicated; **P*<0.05; NS, *P*>0.4). The ratio between spike-induced and plateau potential-induced signals (right) was significantly less than 1 along the somatodendritic length (n as indicated; **P*<0.02, ***P*<0.005, ****P*<0.001). (F) The ratio between burst- and spike-induced calcium signals was reduced at each location after the addition of the ionotropic receptor blockers APV (50 μM), 6-cyano-7-nitroquinoxaline-2,3-dione (20 μM), and bicuculline (3.5-21 μM) (right) compared with control conditions (left) (n as indicated; **P*<0.02).

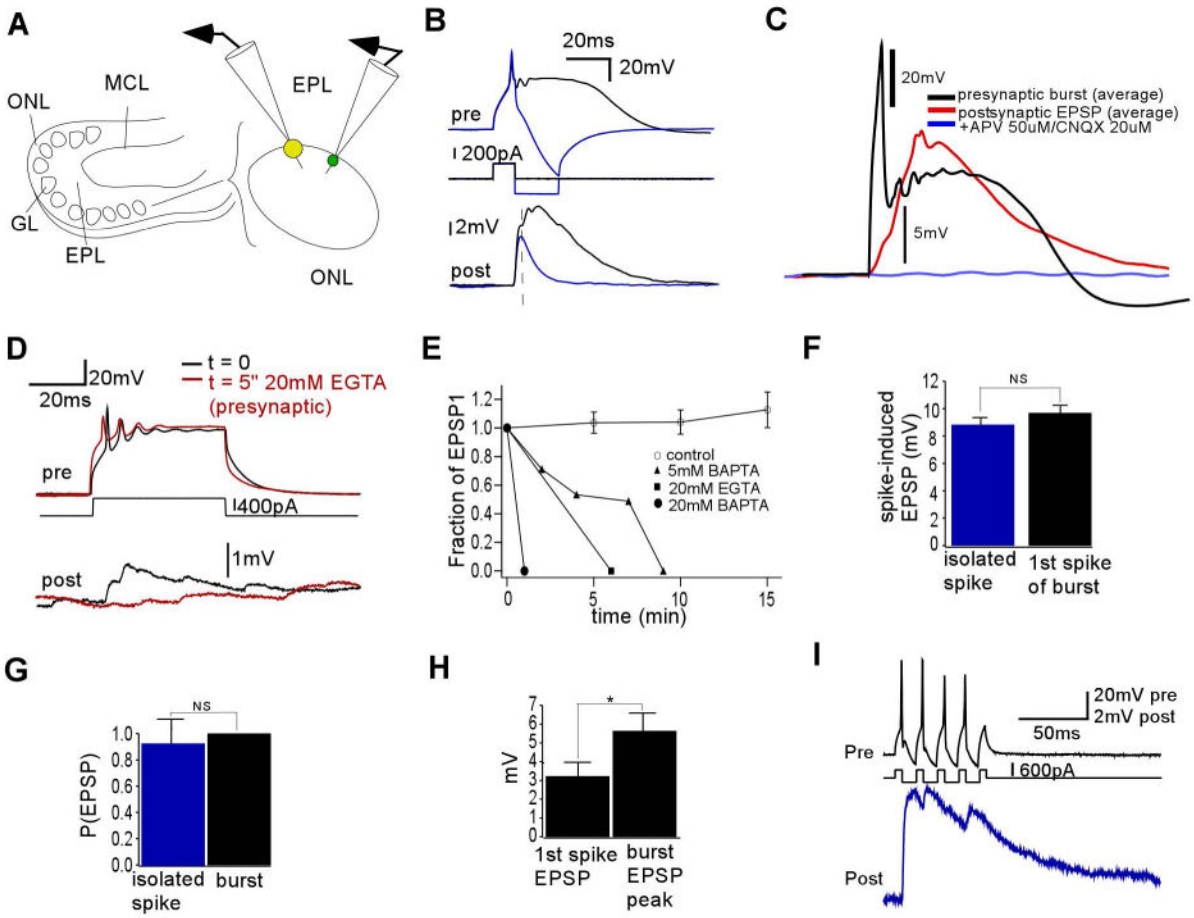

Fig. 3.

Paired whole-cell recordings reveal large, robust monosynaptic excitation by ETC bursts as compared with ETC spikes. (A) Left: Illustration of a horizontal rat OB slice as before. Right: Paired electrical recordings were made between ETCs (larger circle on right) and smaller somata in the glomerular border (smaller circle on right). (B) Presynaptic burst from ETC (above) elicited a large (7.3±4.1 mV, n = 15), long ($t_{half\text{-}max}$ 38±22 ms, n = 15) multicomponent depolarization in the postsynaptic interneuron with monosynaptic delay (below) (0.52±0.19 ms, n = 15). Shown is the average of many trials of a single pair. The preliminary spike (overlaid above) elicited an EPSP (overlaid below) that was similar to the first component of the burst-induced depolarization (n = 7). (C) The burst-induced depolarization was eliminated after the addition of ionotropic glutamate receptor blockers, indicating that it was an EPSP (n = 2). (D) The burst-induced EPSP was eliminated after 5 min of dialysis of presynaptic ETC with a high concentration of calcium chelator (20 mM EGTA) in the intracellular solution. (E) The ETC burst-induced EPSP amplitude, as compared with time t = 0, decayed quickly in time when dialyzed with various chelators but not in control conditions (0.2 mM EGTA). (F) The amplitude of the spike-elicited EPSP was not significantly different from the amplitude of the first component of the burst-induced EPSP (*P*>0.2, similar for all pairs examined, n = 7). (G) The spike-induced EPSP and burst-induced EPSP were both elicited with high probability (n = 7, *P*>0.3). (H) The first spike-

induced EPSP peak was on average significantly smaller than the peak amplitude of the burst-induced EPSP (n = 15, *P<0.02). (I) A train of presynaptic spikes at ∼80 Hz (above) in an ETC–interneuron pair was elicited with alternating depolarizing and hyperpolarizing currents. Resulting EPSPs (below) produced by the train resembled those elicited by the ETC burst.

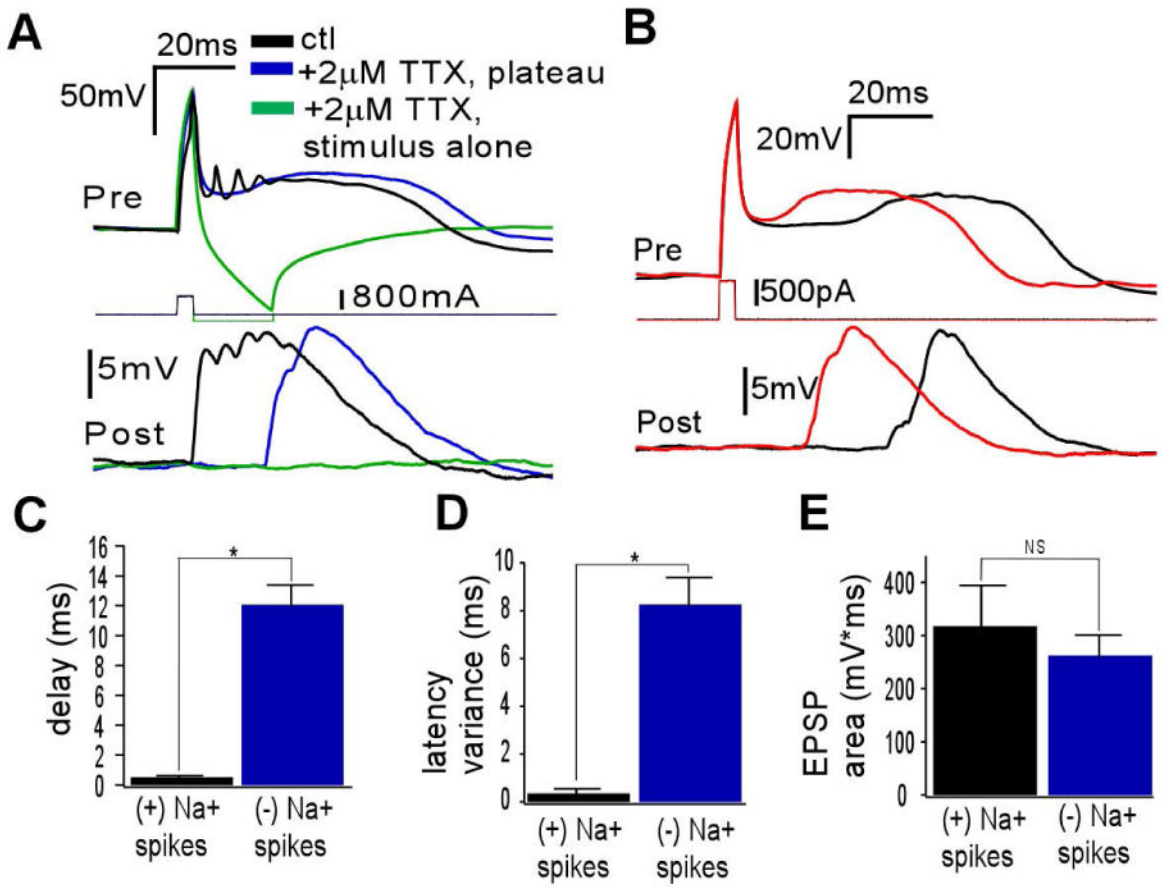

Fig. 4.

The ETC plateau potential robustly elicits large, Na^+ channel-independent EPSPs. (A) ETC (above)/interneuron (below) recordings showing the contribution of the presynaptic ETC burst (ctl), plateau potential (plateau) and capacitative transient (stimulus alone) to excitation in interneurons. Blue and green traces are in the presence of 2 μM TTX (n = 4). The plateau potential produces an EPSP that is similar in duration and amplitude to the burst. The capacitative transient itself produces no EPSP. (B) Single trials of plateau potential-induced excitation show that the EPSP timing varies and shifts with the time course of plateau potential generation. (C) The average synaptic delay of EPSPs induced by bursts (plateau potential and Na^+ spikes) is significantly less than the delay of EPSPs induced by plateau potential in the absence of Na^+ spikes (*P<0.0003). (D) The intertrial variability of the synaptic delay of burst-induced EPSPs is significantly less than that of plateau potential-induced EPSPs (*P<0.0005). (E) The areas of burst- and plateau potential-induced EPSPs were not significantly different (P>0.5).

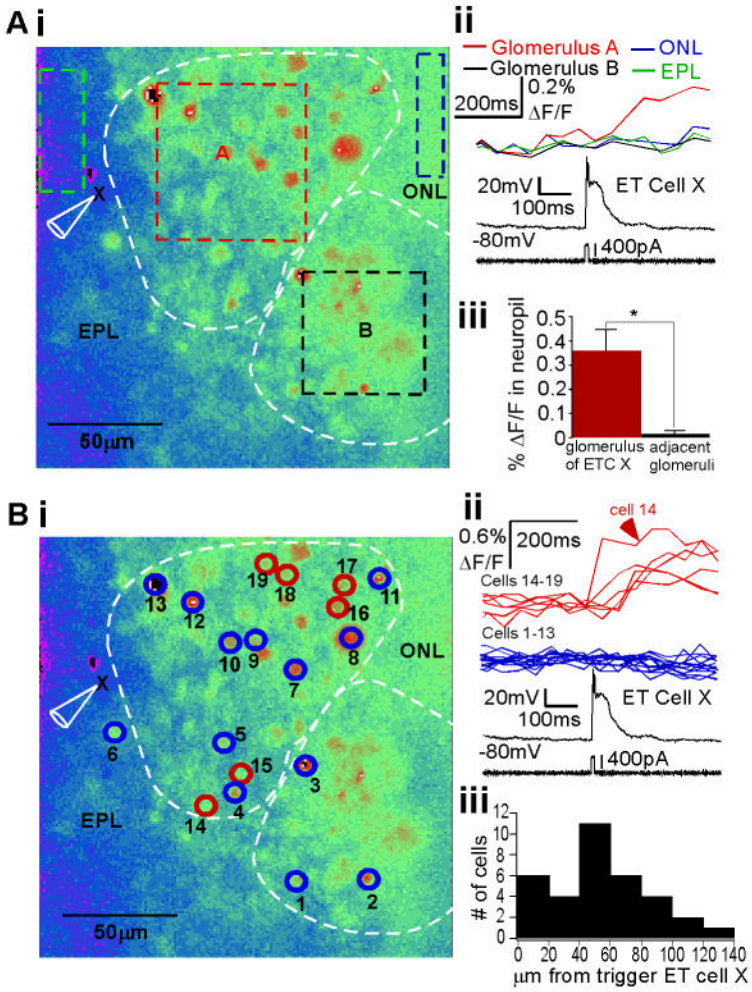

Fig. 5.

An ETC burst promotes spiking in multiple interneurons restricted to one glomerulus. (A) (i) Resting fluorescence image of a horizontal OB slice after incubation with Calcium Green-1 AM dye. The glomerular borders are indicated, and ROIs corresponding to glomerulus A and B, as well as the EPL and olfactory nerve layer (ONL) near to glomerulus A are delineated. The recorded ETC of glomerulus A is labeled (X). (ii) The ETC was stimulated via whole-cell patch (no dye in electrode) to fire one burst (bottom). The neuropil signal (ΔF/F) is shown above, demonstrating that only glomerulus A generated a measurable signal. (iii) Over all experiments, neuropil fluorescence in the glomerulus of ETC X was significantly increased over that of neighboring glomeruli (n = 11 slices, $P<0.0001$). (B) Cellular level analysis. (i) Same slice as in A. Neuronal somata ROIs are indicated with circles and numbers, representing responsive and some unresponsive somata. (ii) Overlay of somatic signal from neurons that were responsive (top) or unresponsive (middle) to a burst simulated in ETC X (bottom), with number identification noted. Note that responsive cells are restricted to glomerulus A. (iii) Histogram of distance between follower interneurons and trigger ETCs over several experiments (n = 6 slices). Responsive cells were restricted to distances within the typical range of glomerular diameters (100-150 μm).

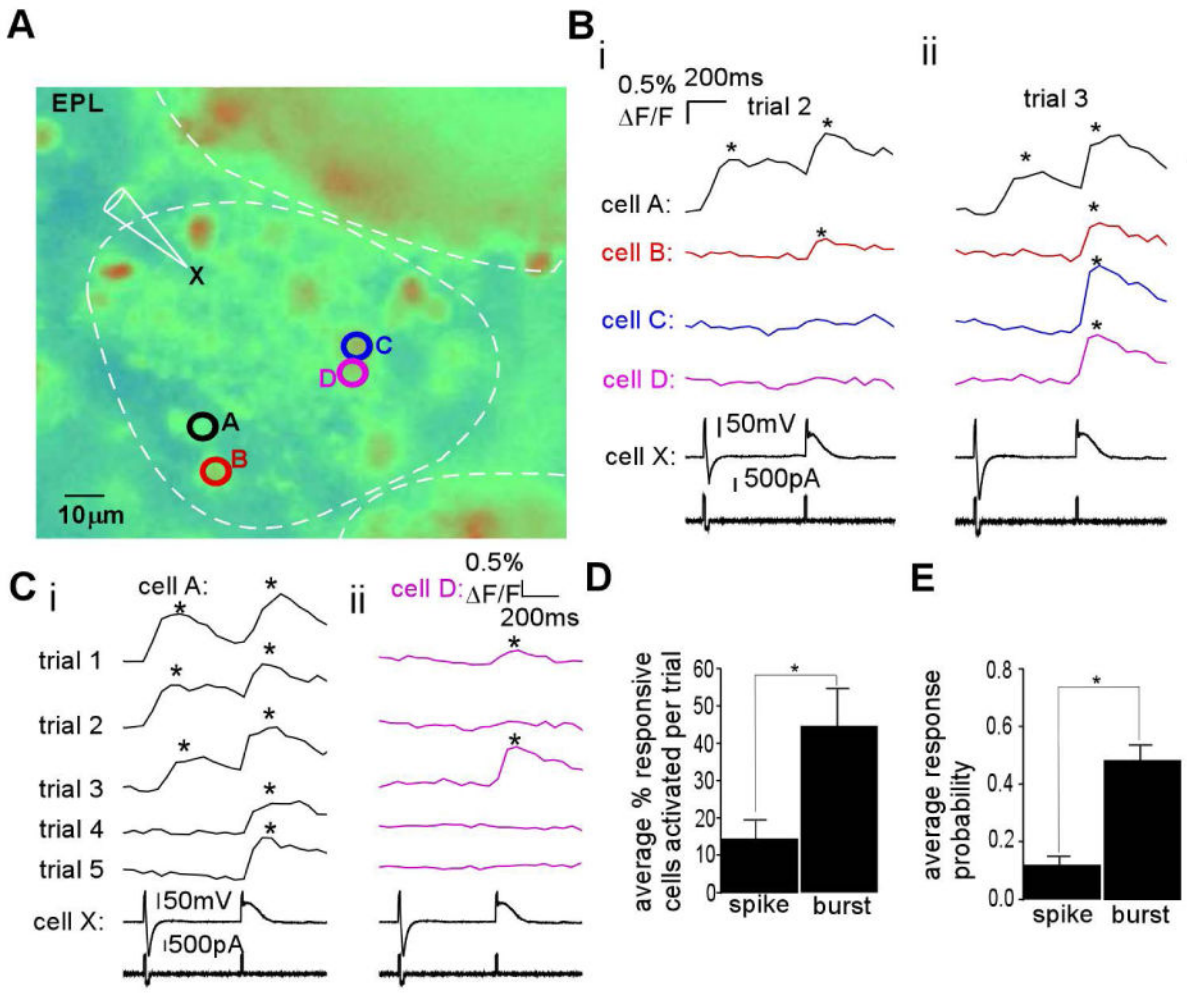

Fig. 6.

An ETC burst promotes intraglomerular coactivity better than single spikes. (A) Resting fluorescence image of a Calcium Green-1 AM dye-loaded OB slice with trigger ETC X and responsive interneurons A-D indicated. (B) In a single trial, both a single spike and a burst were elicited in ETC X, separated by 500 ms (i and ii, "cell X", at bottom), and fluorescence transients were monitored in interneurons A-D (i and ii, above electrical trace). (i) In trial 2, the spike triggered a response in cell A, whereas the plateau triggered a response in both cells A and B. (ii) In another separate trial (trial 3), the spike only triggered a response in cell A, whereas the burst triggered a response in all four cells. (C) (i) In multiple repeated trials, using the same stimulation protocol, and focusing on responses in cell A, the single spike triggered a response in 3/5 trials, whereas the burst triggered a response in 5/5 trials. (ii) For cell D, the burst elicited a response in 2/5 trials, whereas the spike was not successful in any of the trials. (D) In such experiments (n = 6 slices), the ability to coactivate multiple interneurons was calculated as the average percent of responding cells activated per trial. This value was significantly increased by burst firing vs. spike firing (**P*<0.03). (E) For a given follower interneuron, burst firing in trigger ETC X was significantly more likely to elicit a response than a single spike (n = 32, **P*<0.0001).